

## Supporting Information

*“Amyloid-like behaviour of site-specifically citrullinated myelin oligodendrocyte protein (MOG) peptide fragments inside EBV infected B-cells influences their cytotoxicity and autoimmunogenicity.”*

Can Araman,<sup>†,\*</sup> Miriam E. van Gent,<sup>†</sup> Nico J. Meeuwenoord,<sup>‡</sup> Nicole Heijmans,<sup>§</sup> Mikkel H.S. Marqvorsen,<sup>†</sup> Ward Doelman,<sup>†</sup> Bart W. Faber,<sup>⊥</sup> Bert A. 't Hart,<sup>§,¶,\*</sup> Sander I. Van Kasteren<sup>†,\*</sup>

<sup>†</sup>Leiden Institute of Chemistry and the Institute for Chemical Immunology, Leiden University, Einsteinweg 55, 2333 CC Leiden, The Netherlands.

<sup>‡</sup>Leiden Institute of Chemistry and Department of Bioorganic Synthesis, Leiden University, Einsteinweg 55, 2333 CC Leiden, The Netherlands.

<sup>§</sup>Dept. Immunobiology, Biomedical Primate Research Centre, Rijswijk, The Netherlands

<sup>⊥</sup>Dept. Parasitology, Biomedical Primate Research Centre, Rijswijk, The Netherlands

<sup>¶</sup>University of Groningen, Dept. Neuroscience, University Medical Centre, Groningen, The Netherlands

### Corresponding authors

C. Araman (m.c.araman@lic.leidenuniv.nl), B.A. 't Hart (hart@bprc.nl), S.I. van Kasteren (s.i.van.kasteren@chem.leidenuniv.nl)

## **Chemicals**

Chemical reagents for buffer preparation, organic synthesis, SPPS and solvents for HPLC-purification were purchased from Acros (Belgium), Biosolve (the Netherlands), Chem-Lab (Belgium), Honeywell Riedel-de Haën (Germany), Merck (The Netherlands), Novabiochem (The Netherlands), Sigma Aldrich (The Netherlands), Sigma Life Sciences (The Netherlands) or Sphaero Hispanagar (Spain) and used without further purification unless stated otherwise. Following fluorescent molecules were purchased by commercial sources within the Netherlands: Alexa Fluor 488 Azide and Alexa Fluor 647 Azide (Thermo Fisher Scientific, Amsterdam). Tentagel S RAM and Tentagel S HMBA resins were purchased from Rapp Polymere GmbH (Germany). Fluorenylmethoxycarbonylchloride (Fmoc) protected amino acids with following protecting groups, Fmoc-Gly-OH, Fmoc-Leu-OH, Fmoc-Val-OH, Fmoc-Phe-OH, Fmoc-Glu(OtBu)-OH, Fmoc-Ala-OH, Fmoc-Ile-OH, Fmoc-Met-OH and Fmoc-Cit-OH were obtained from NovaBiochem (Germany). Fmoc-Tyr(tBu)-OH was obtained from Bachem AG (Germany), whereas Fmoc-Asp(OtBu)-OH, Fmoc-Gln(Trt)-OH, Fmoc-Lys(Boc)-OH, Fmoc-Asn(Trt)-OH, Fmoc-Arg(Pbf)-OH, Fmoc-His(Trt)-OH, Fmoc-Ser(tBu)-OH, Fmoc-Pro-OH and Fmoc-Trp(Boc)-OH were bought from Sigma Aldrich (Germany). *N,N*-Diisopropylethylamine (DIPEA) and 2-(6-Chloro-1H-benzotriazole-1-yl)-1,1,3,3-tetramethylaminium hexafluorophosphate (HCTU) were obtained from Carl Roth GmbH (Germany) and Novabiochem (Germany) respectively.

## **Cloning, expression and purification of rMOG<sub>1-125</sub>**

The pUC57 plasmid (ampicillin resistance) containing the insert MOG1-125 coding sequence as well as NcoI and NotI restriction sites and a lac promoter was purchased by BaseClear B.V. (the Netherlands). The His<sub>10</sub>-TEV pET28a vector with kanamycin resistance contained NcoI and NotI restriction sites after His<sub>10</sub> and TEV coding sequence, the T7lac promoter and terminator. Following forward and reverse primers were used for subcloning: 5'-ATAACCATGGGGCATGGGTCAGTTCCG-3' and 5'-CGCGGCCGCTTAGCCCGGAG-3'. The insert was amplified using standard PCR protocols, purified via PCR purification kit (Qiagen, USA)

and subjected to restriction with NcoI and NotI, while the vector was restricted with the same restriction enzymes. Insert and vector were ligated at 22°C o.n. The ligation mixture was transformed into *E. coli* XL-10, grown on an LB-agar-plate (50 µg/mL Kanamycin and 50 µg/mL Ampicillin), colonies were selected and analyzed via colony PCR. Selected clones were sequenced with T7-promotor and T7-terminator primers at the Leids Universitair Medisch Centrum (LUMC).

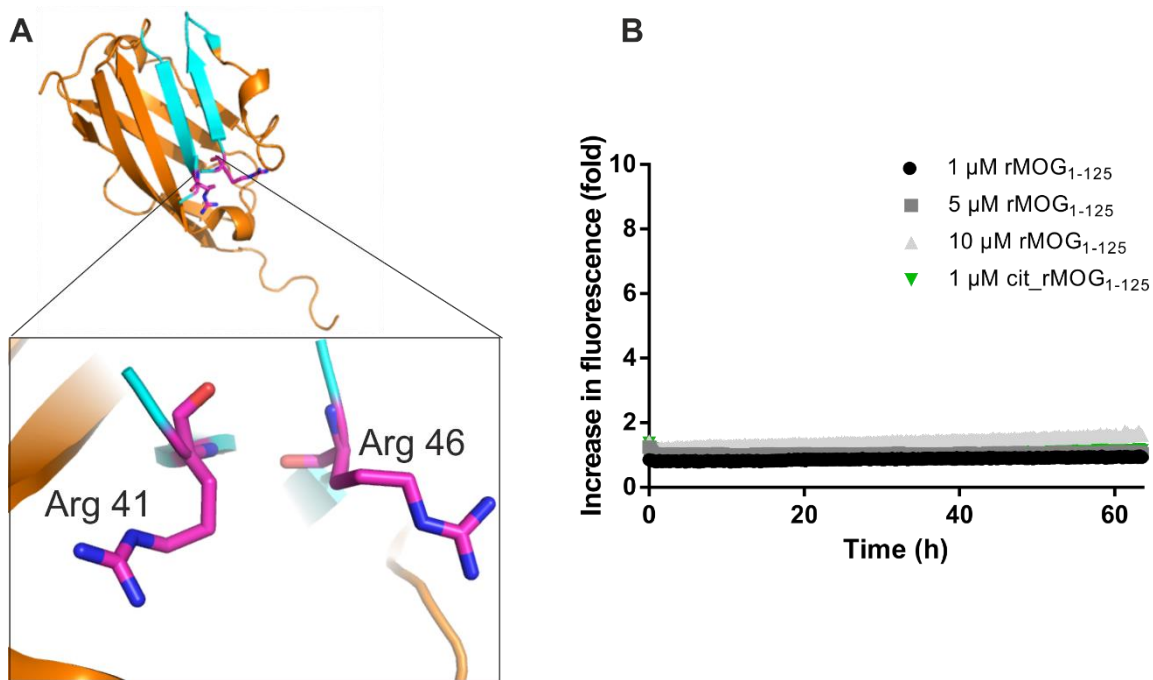
*E. coli* ROS2DE3 competent cells were transformed with 100 ng of ligation product. A colony was selected to grow o.n. in 5 mL LB for medium containing 2 µL (50 µg/mL) kanamycin and 5 µL chloramphenicol (25µg/mL) at 37 °C. Next, glycerol stocks were prepared, and cells were cultured o.n. from the glycerol stocks in 10 mL LB for medium (Kan<sup>R</sup>/Cam<sup>R</sup>) at 37 °C. Fresh LB-medium was inoculated with the o.n. culture in a 1:10 (v/v) ratio. When the cells reached the log-phase (OD<sub>600</sub>≥0.6) the expression was induced by the addition of 1mM isopropyl β-D-1-thiogalactopyranoside (IPTG, 0.5 M stock solution). The cells were left to grow at 37 °C during the day following reduction of the temperature to 30 °C o.n. Samples were collected before and after induction with IPTG at several time points and stored at -20 °C for further use.

Upon o.n. incubation, cells were harvested (3500 g, 4 °C for 20-40 min), the supernatant was removed and washed once with 20 mL of lysis buffer (50mM Tris, 300 mM NaCl, pH 8.5). Supernatant was discarded, and pellet was dissolved in 10 mL lysis buffer. Cells were lysed using the Stansted Pressure Cell Homogenizer and centrifuged at 10000 rpm, 4 °C for 1-2 h. Supernatant and pellet were separated and analyzed via SDS-PAGE. The protein was expressed in inclusion bodies, following steps were followed to solubilize the protein of interest; fractions were washed with 20 mL lysis buffer with Triton-X (0.05-0.1%) and centrifuged at 10000 rpm, 4 °C for 1.5 h. Subsequently, the supernatant was discarded, and 20 mL of lysis buffer was added to the pellet, mixed and centrifuged down at 10000 rpm, 4 °C for 1 h twice. Then, the pellet was collected and homogenized in solubilization buffer (6M Urea, 50mM Tris, 300 mM NaCl, pH 8.5)

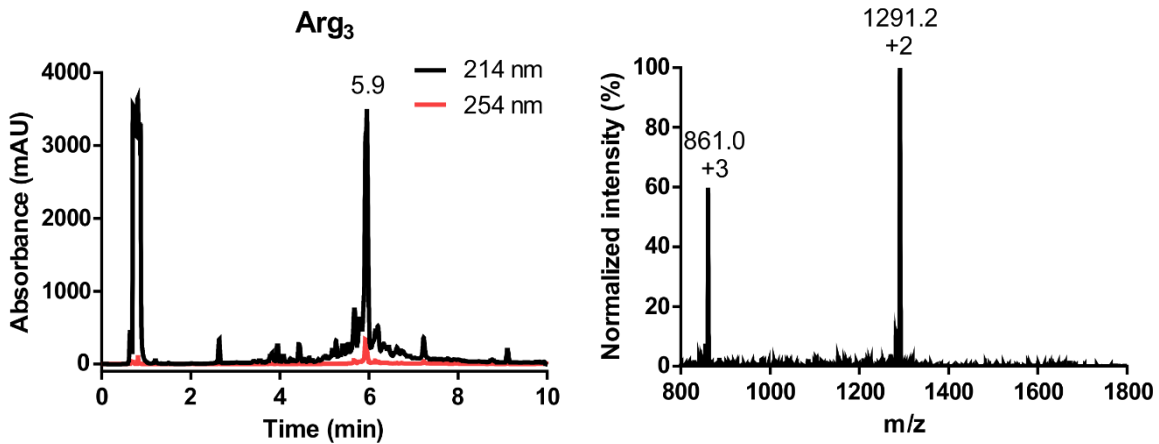
o.n. at RT. The next day, the samples were centrifuged at 10000 rpm, 4 °C for 2 h, the supernatant was transferred to a new tube and stored for further purification.

The protein sample was purified over a HisPur Ni-NTA resin (Thermo Scientific) using manufacturer's protocols. Washing steps were performed using solubilization buffer supplied with imidazole in increasing concentrations (10-50 mM Imidazole final concentration). Elution was achieved with solubilization buffer supplemented with 250 mM imidazole.

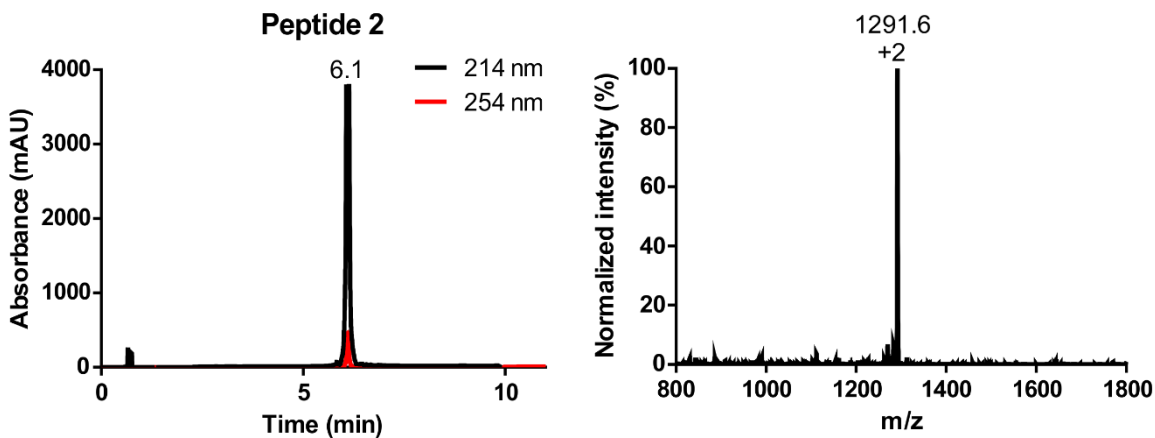
The elution fraction was desalted by gel filtration using 2 mL Thermo Scientific Zeba™ Spin Desalting Columns. Desalting buffer (6M Urea in 50 mM Tris, 300 mM NaCl, pH 8.5) was used to wash the column. Desalted samples were further diluted and subsequently dialyzed to enable refolding. Stepwise dilution refolding was done by adding a respective volume of refolding buffer (50 mM Tris, 300 mM NaCl, pH 8.5) to the desalted protein solution in urea containing buffer at 4 °C. Following dilution strategy was used; 6M → 5M → 4M → 3M → 2M → 1M → 0.5M Urea (each step 1-2 h incubation after dilution). Refolded samples were dialyzed to storage buffer (50 mM Tris, 300 mM NaCl, pH 8.5), frozen in liquid nitrogen and stored at -80°C for further use. Samples were characterized via LC-MS and CD spectroscopy (Supplementary Fig. 21). If required, rMOG<sub>1-125</sub> was citrullinated with recombinant PAD4 (Sigma Aldrich) according to manufacturer's recommendations.



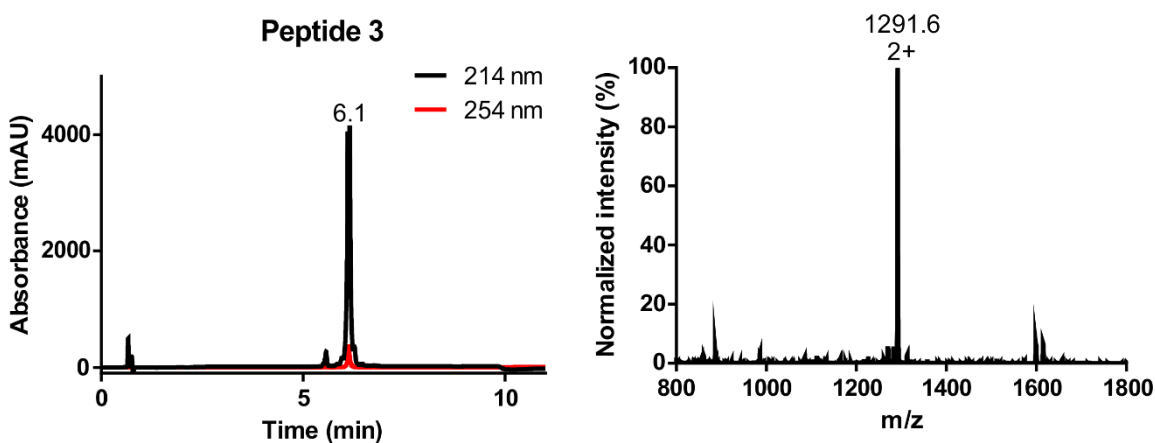
**Supporting Figure 1:** ThT Aggregation Assay of recombinant FL-MOG (rMOG1-125) and citrullinated FL-MOG (cit\_rMOG) at different concentrations (varying from 1-10  $\mu\text{M}$ ). PBD-ID: 1PKO



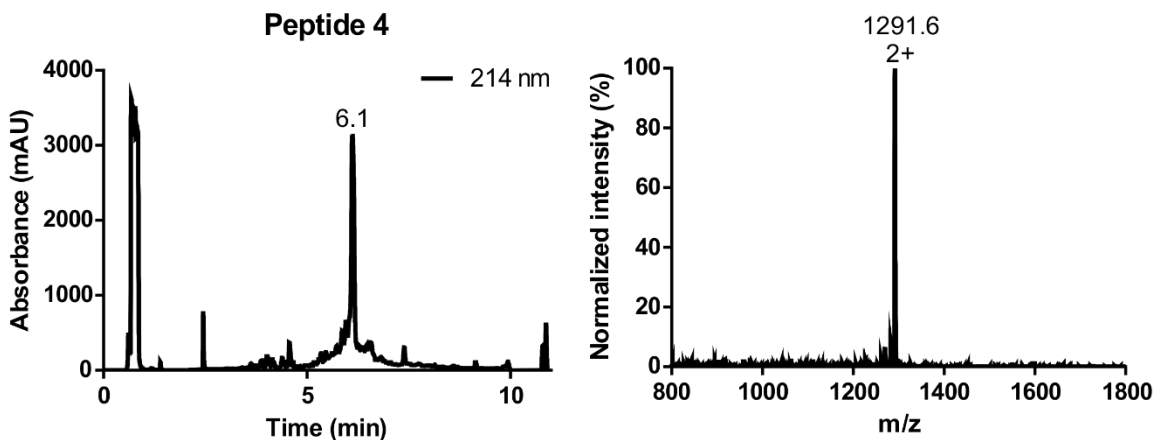
**Supporting Figure 2: Characterization of Peptide 1 ( $\text{Arg}_3$ ).** Left panel: analytical C18 RP-HPLC chromatogram of purified Peptide 1 ( $\text{Arg}_3$ ), linear gradient 10-90% ACN. Right panel: corresponding mass spectrum of Peptide 1 ( $\text{Arg}_3$ ) at  $t = 5.9$  min, expected mass: 2579.3 Da, observed mass: 2580.4 Da  $[\text{M}+\text{H}]^+$ , 1291.2  $[\text{M}+2\text{H}]^{2+}$ , 861.0  $[\text{M}+3\text{H}]^{3+}$ .



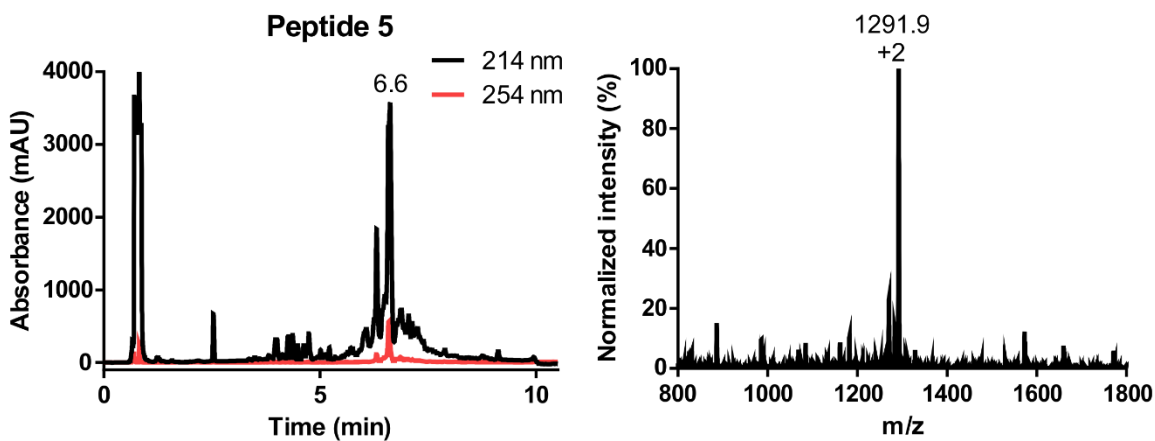
**Supporting Figure 3: Characterization of peptide 2.** Left panel: analytical C18 RP-HPLC chromatogram of purified Peptide 2, linear gradient 10-90% ACN. Right panel: corresponding mass spectrum of Peptide 2 at  $t = 6.1$  min, expected mass: 2580.3 Da, observed mass: 2581.2 Da  $[M+H]^+$ , 1291.6  $[M+2H]^{2+}$ .



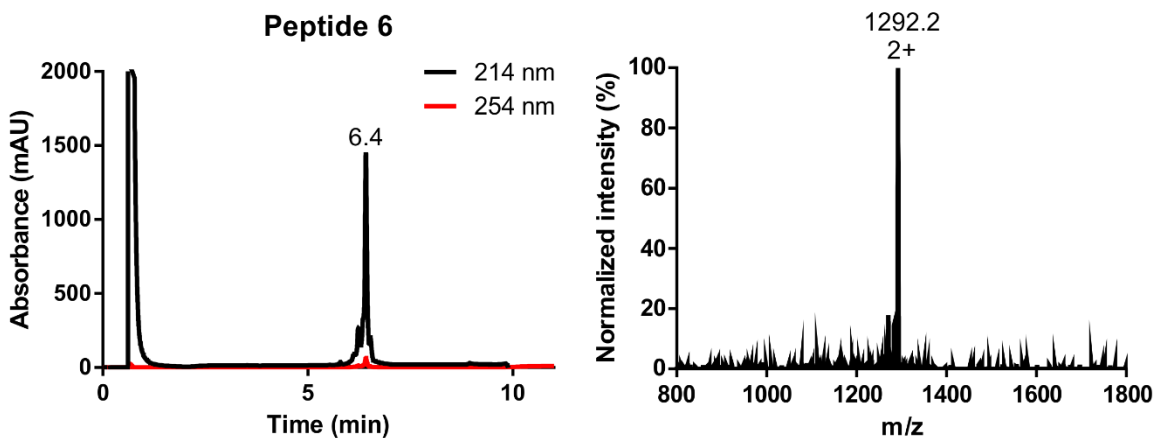
**Supporting Figure 4: Characterization of peptide 3.** Left panel: analytical C18 RP-HPLC chromatogram of purified Peptide 3, linear gradient 10-90% ACN. Right panel: corresponding mass spectrum of Peptide 3 at  $t = 6.1$  min, expected mass: 2580.3 Da, observed mass: 2581.2 Da  $[M+H]^+$ , 1291.6  $[M+2H]^{2+}$ .



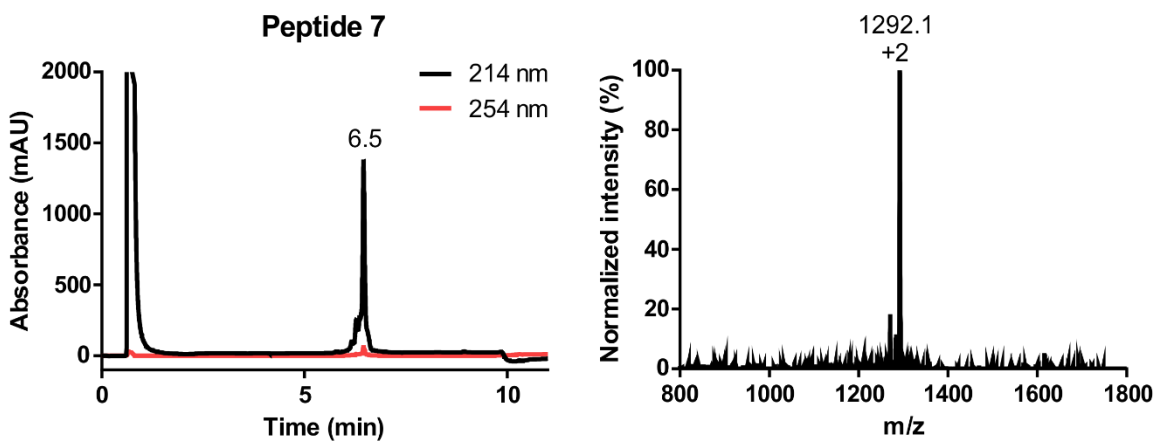
**Supporting Figure 5: Characterization of peptide 4.** Left panel: analytical C18 RP-HPLC chromatogram of purified Peptide 4, linear gradient 10-90% ACN. Right panel: corresponding mass spectrum of Peptide 4 at  $t = 6.1$  min, expected mass: 2580.3 Da, observed mass: 2581.2 Da  $[M+H]^+$ , 1291.6  $[M+2H]^{2+}$ .



**Supporting Figure 6: Characterization of peptide 5.** Left panel: analytical C18 RP-HPLC chromatogram of purified Peptide 5, linear gradient 10-90% ACN. Right panel: corresponding mass spectrum of Peptide 5 at  $t = 6.6$  min, expected mass: 2581.3 Da, observed mass: 2583.8 Da  $[M+H]^+$ , 1291.9  $[M+2H]^{2+}$ .

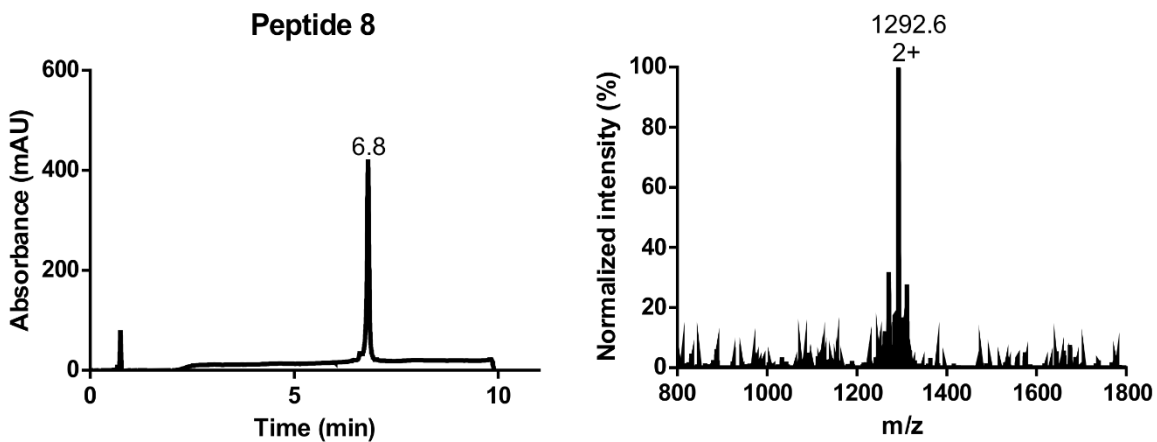


**Supporting Figure 7: Characterization of peptide 6.** Left panel: analytical C18 RP-HPLC chromatogram of purified Peptide 6, linear gradient 10-90% ACN. Right panel: corresponding mass spectrum of Peptide 6 at  $t = 6.4$  min, expected mass: 2581.3 Da, observed mass: 2584.4 Da  $[M+H]^+$ , 1292.2  $[M+2H]^{2+}$ .

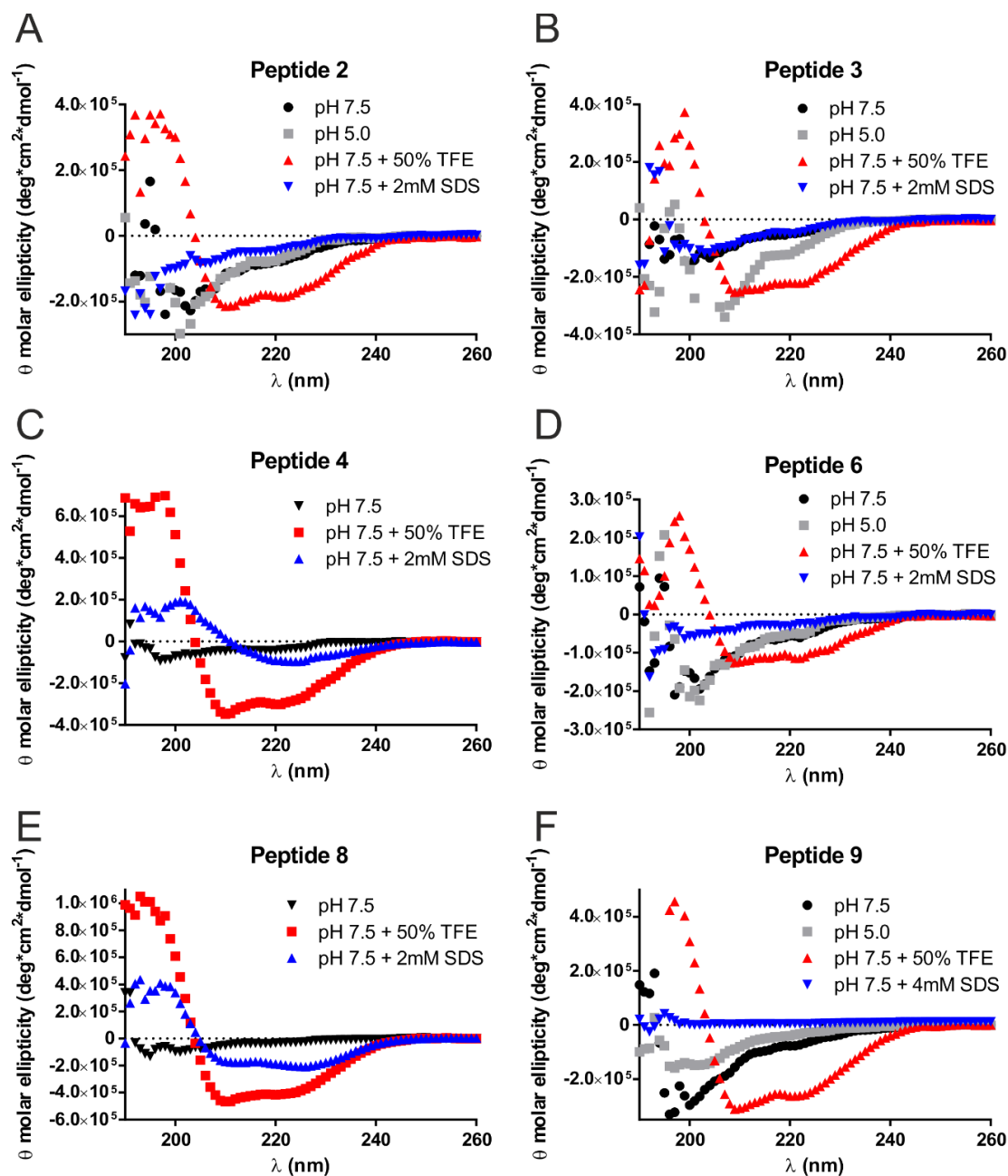


**Supporting Figure 8: Characterization of peptide 7.** Left panel: analytical C18 RP-HPLC chromatogram of purified Peptide 7, linear gradient 10-90% ACN. Right panel: corresponding mass spectrum of Peptide 7 at  $t = 6.5$  min, expected mass: 2581.3 Da, observed mass: 2584.2 Da  $[M+H]^+$ , 1292.1  $[M+2H]^{2+}$ .

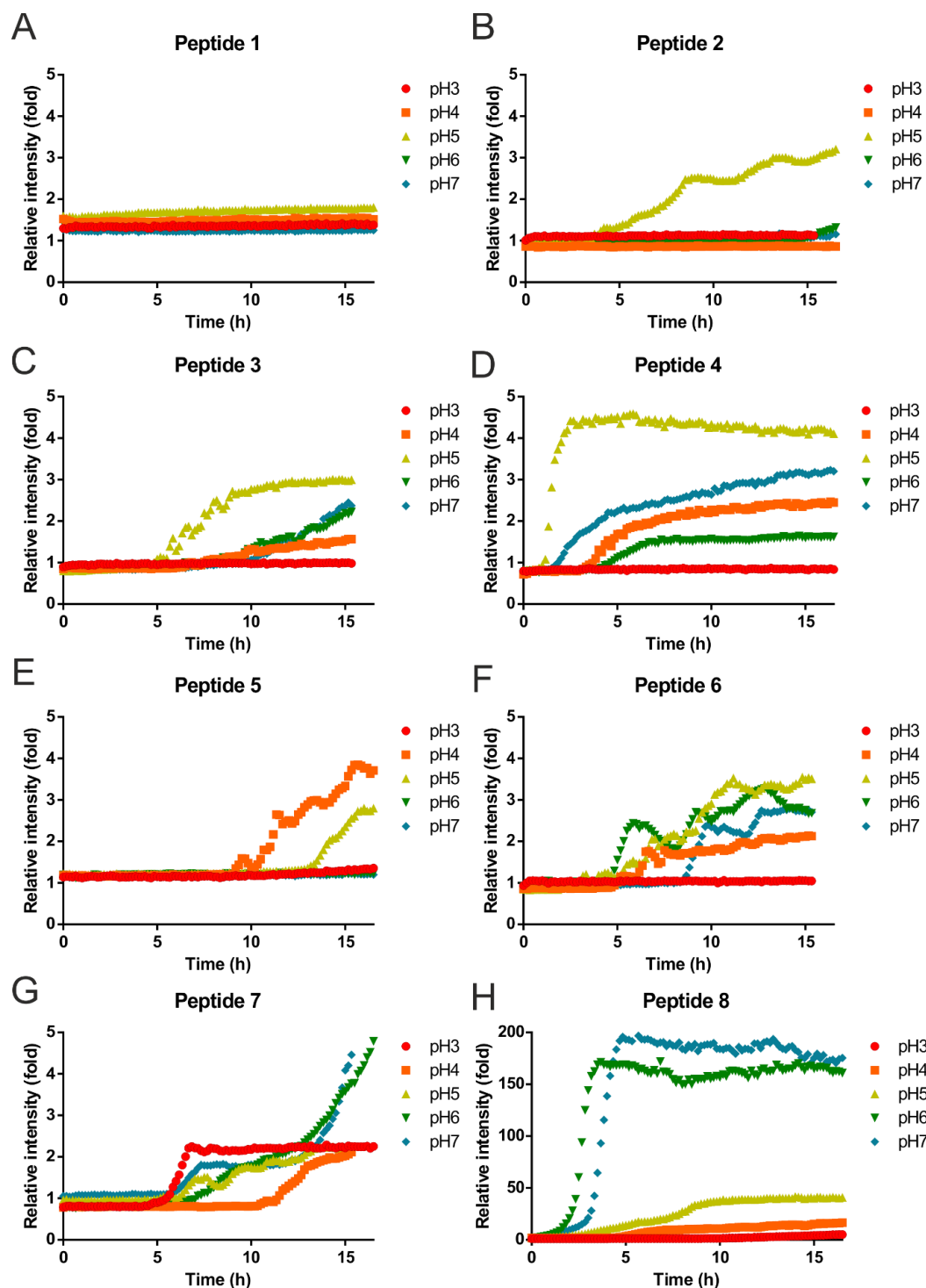




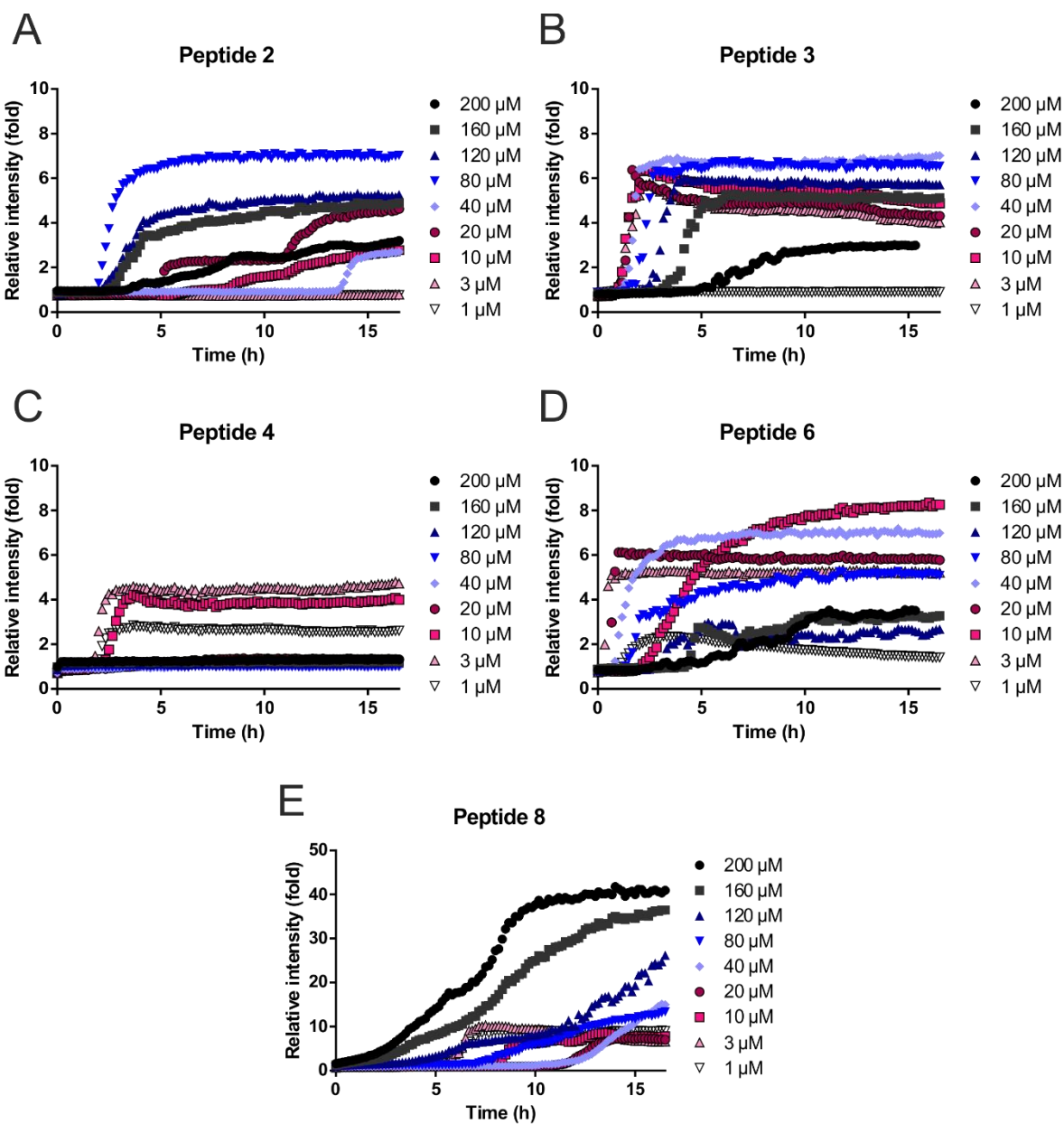
**Supporting Figure 9: Characterization of peptide 8.** Left panel: analytical C18 RP-HPLC chromatogram of purified Peptide 8, linear gradient 10-90% ACN. Right panel: corresponding mass spectrum of Peptide 6 at  $t=6.4$  min, expected mass: 2582.3 Da, observed mass: 2585.2 Da  $[M+H]^+$ , 1292.6  $[M+2H]^{2+}$ .



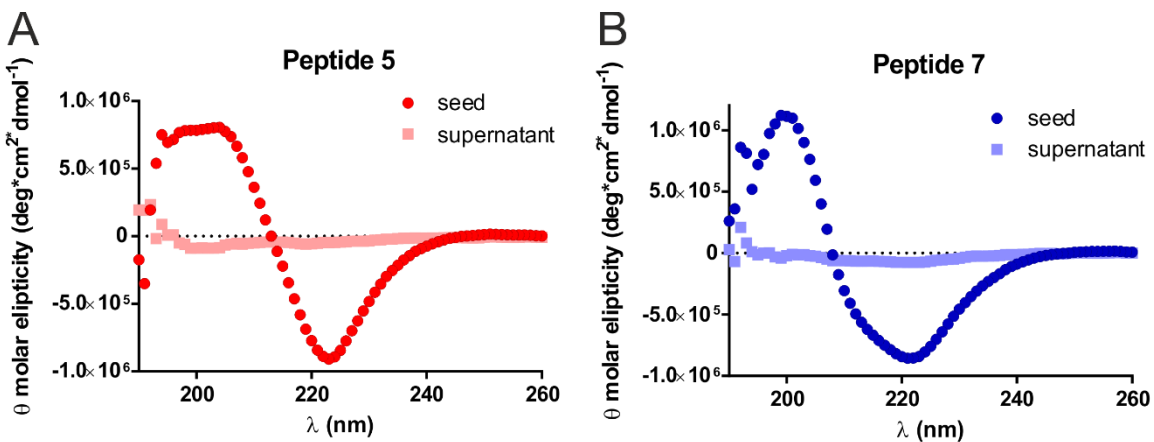
**Supporting Figure 10: Biophysical characterization of peptides 2-4, 6, 8 and 9 via CD spectroscopy.** A: CD spectra of 2 at different pH (5.0 and 7.5) and with additives (TFE and SDS), [c]=50  $\mu$ M (0.13 mg/mL), B: CD spectra of 3 at different pH (5.0 and 7.5) and with additives (TFE and SDS), [c]=50  $\mu$ M, C: CD spectra of 4 at different pH (5.0 and 7.5) and with additives (TFE and SDS), [c]=50  $\mu$ M, D: CD spectra of 6 at different pH (5.0 and 7.5) and with additives (TFE and SDS), [c]=50  $\mu$ M, E: CD spectra of 8 at different pH (5.0 and 7.5) and with additives (TFE and SDS), [c]=50  $\mu$ M, F: CD spectra of 9 at different pH (5.0 and 7.5) and with additives (TFE and SDS), [c]=50  $\mu$ M. All spectra were recorded from 190-260 nm. black circles: sample in 20 mM Tris Buffer (pH 7.5), grey squares: sample in 20 mM Sodiumacetate (NaOAc) buffer, red triangles: sample treated with 50% (v/v) TFE as an  $\alpha$ -helix enhancer, blue triangles: sample treated with micellar concentrations of SDS (2-4 mM) as  $\beta$ -sheet inducer.



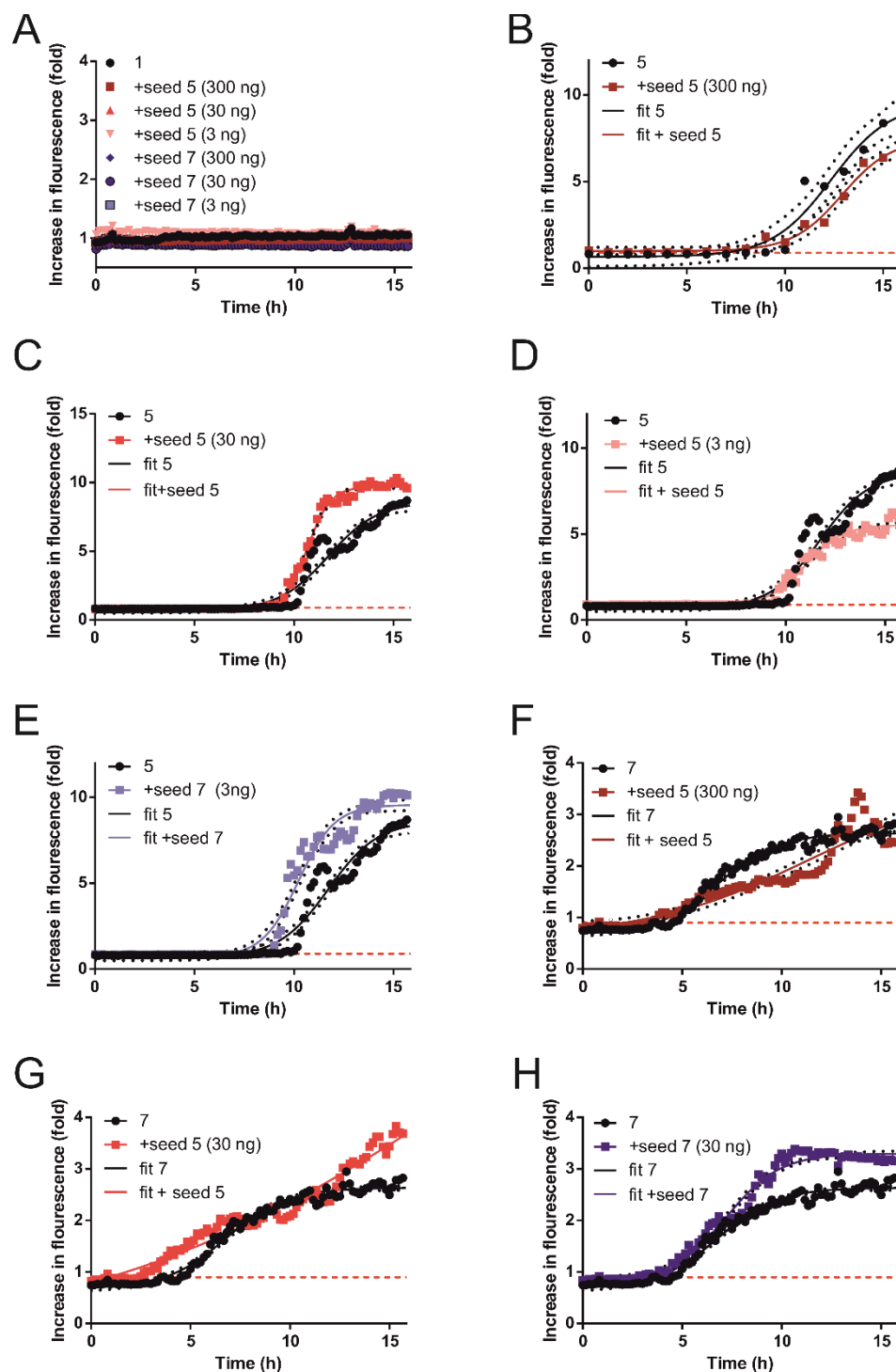
**Supporting Figure 11: ThT fluorescence measured at 37°C at different pH with NaOAc buffer.** All data were recorded at an excitation wavelength of  $444\pm 9$  nm and an emission wavelength of  $485\pm 9$  nm. All samples were used at a concentration of 0.5 mg/mL ( $\sim 200$   $\mu$ M). Red circles: pH 3, orange squares: pH 4, yellow triangle: pH 5, green triangles: pH 6, blue diamonds: pH 7, A-H: fluorescence spectrum of peptides 1-8. The fluorescence change is normalized to 20 mM NaOAc (pH 5) treated with equal amount of ThT as in the samples.



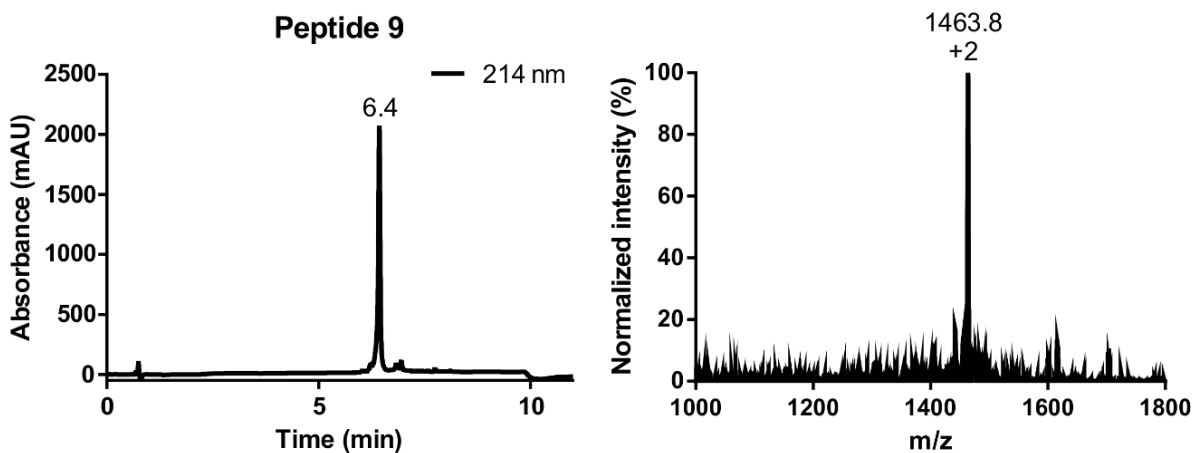
**Supporting Figure 12: ThT fluorescence measured at 37°C, pH 5.0 at different concentrations.** All data were recorded at an excitation wavelength of  $444\pm 9$  nm and an emission wavelength of  $485\pm 9$  nm. All samples were used at a pH of 5.0 with varying concentrations. Black circles: 200  $\mu\text{M}$ , grey squares: 160  $\mu\text{M}$ , dark blue triangle: 120  $\mu\text{M}$ , light blue triangles: 80  $\mu\text{M}$ , purple diamonds: 40  $\mu\text{M}$ , red circles: 20  $\mu\text{M}$ , red squares: 10  $\mu\text{M}$ , pink triangle: 3  $\mu\text{M}$  and white triangle: 1  $\mu\text{M}$ , A-E: fluorescence spectrum of peptides **2**, **3**, **4**, **6** and **8** respectively. The fluorescence change is normalized to 20 mM NaOAc (pH 5) treated with equal amount of ThT as in the samples.



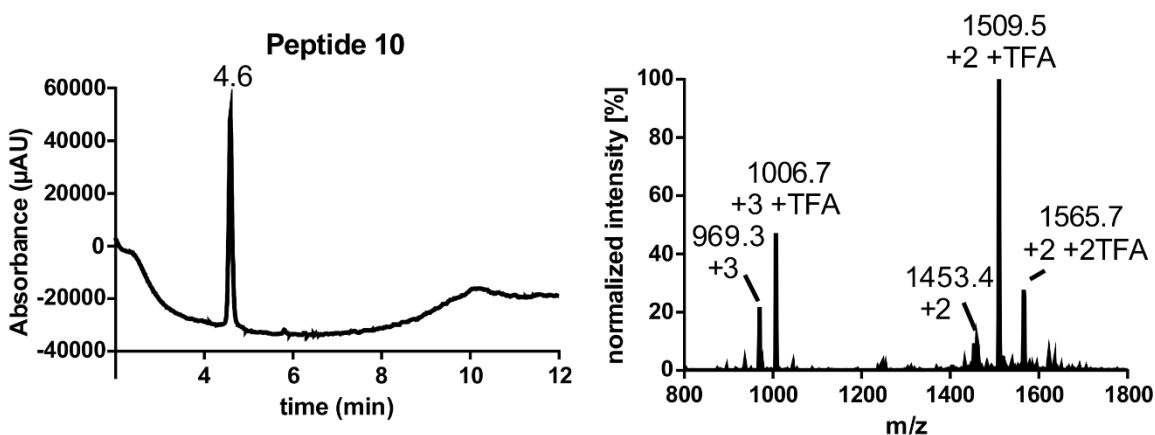
**Supporting Figure 13: CD spectroscopy of seeds from 5 and 7.** The seeds were generated via incubation of the peptide at 37°C (pH 5.0, 20  $\mu\text{M}$ ) for 48h and separated from the supernatant via centrifugation. Pellet was homogenized in 20 mM NaOAc (pH 5.0) at 20  $\mu\text{M}$  concentration. All spectra were recorded with an average of 5 single spectrum and measured at 190-260 nm.



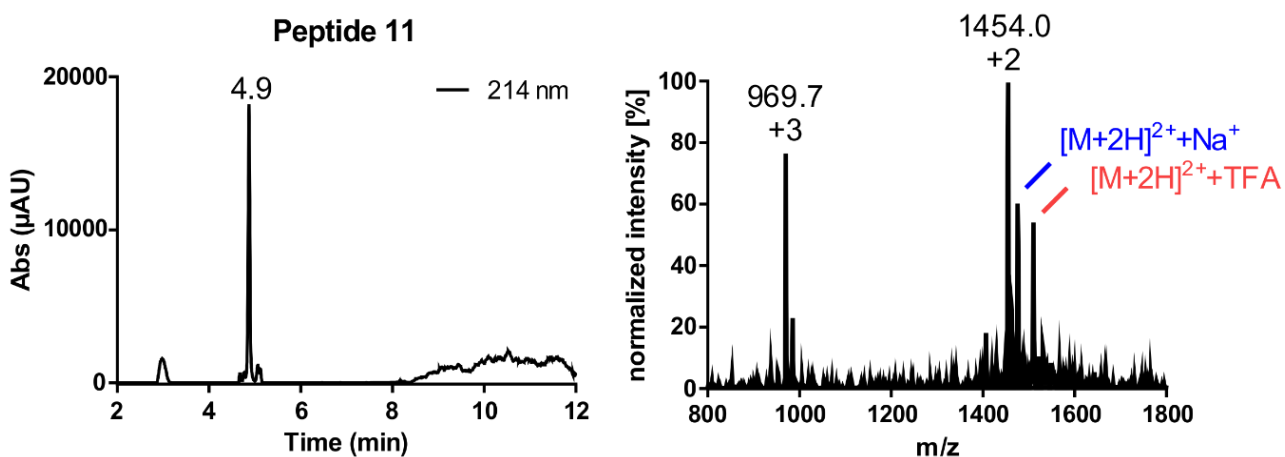
**Supporting Figure 14: Seeded aggregation of peptides 5 and 7.** Peptides 1, 5 and 7 were subjected to aggregation in the presence of seeds from either peptide 5 (depicted as „seed 5“) or 7 (depicted as „seed 7“) with different amounts (3, 30 and 300 ng in 200  $\mu$ L). For aggregation-prone peptides 5 and 7, aggregation curves were fitted (depicted as „fit“, also see Equation E1 in Supporting Information) to determine the change in  $t_{1/2}$  as a measure of aggregation kinetics. All data were recorded at an excitation wavelength of  $444\pm 9$  nm and an emission wavelength of  $485\pm 9$  nm. All samples were used at a pH of 5.0 and 20  $\mu$ M.



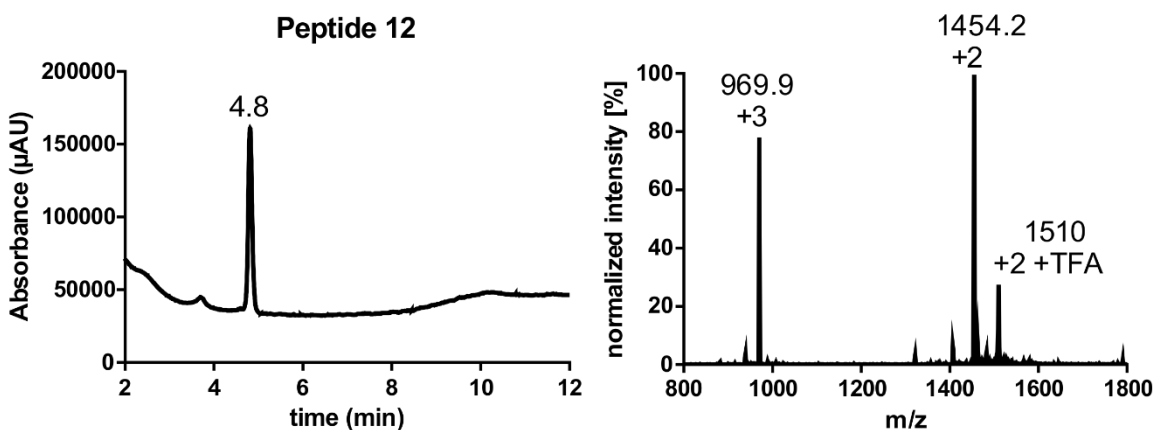
**Supporting Figure 15: Characterization of peptide 9.** Left panel: analytical C18 RP-HPLC chromatogram of purified Peptide 9, linear gradient 10-90% ACN. Right panel: corresponding mass spectrum of Peptide 12 at  $t = 6.4$  min, expected mass: 2925.3 Da, observed mass: 2925.6 Da  $[M+H]^+$ , 1463.8  $[M+2H]^{2+}$ .



**Supporting Figure 16: Characterization of peptide 10.** Left panel: analytical C18 RP-HPLC chromatogram of purified Peptide 10, linear gradient 10-90% ACN. Right panel: corresponding mass spectrum of Peptide 10 at  $t = 4.6$  min, expected mass: 2906.6 Da, observed mass: 2904.9 Da  $[M+H]^+$ , 1453.4  $[M+2H]^{2+}$ , 969.3  $[M+3H]^{3+}$ . Mono- (3017 Da) and di-TFA (3129.4 Da) salt of the peptide were obtained.

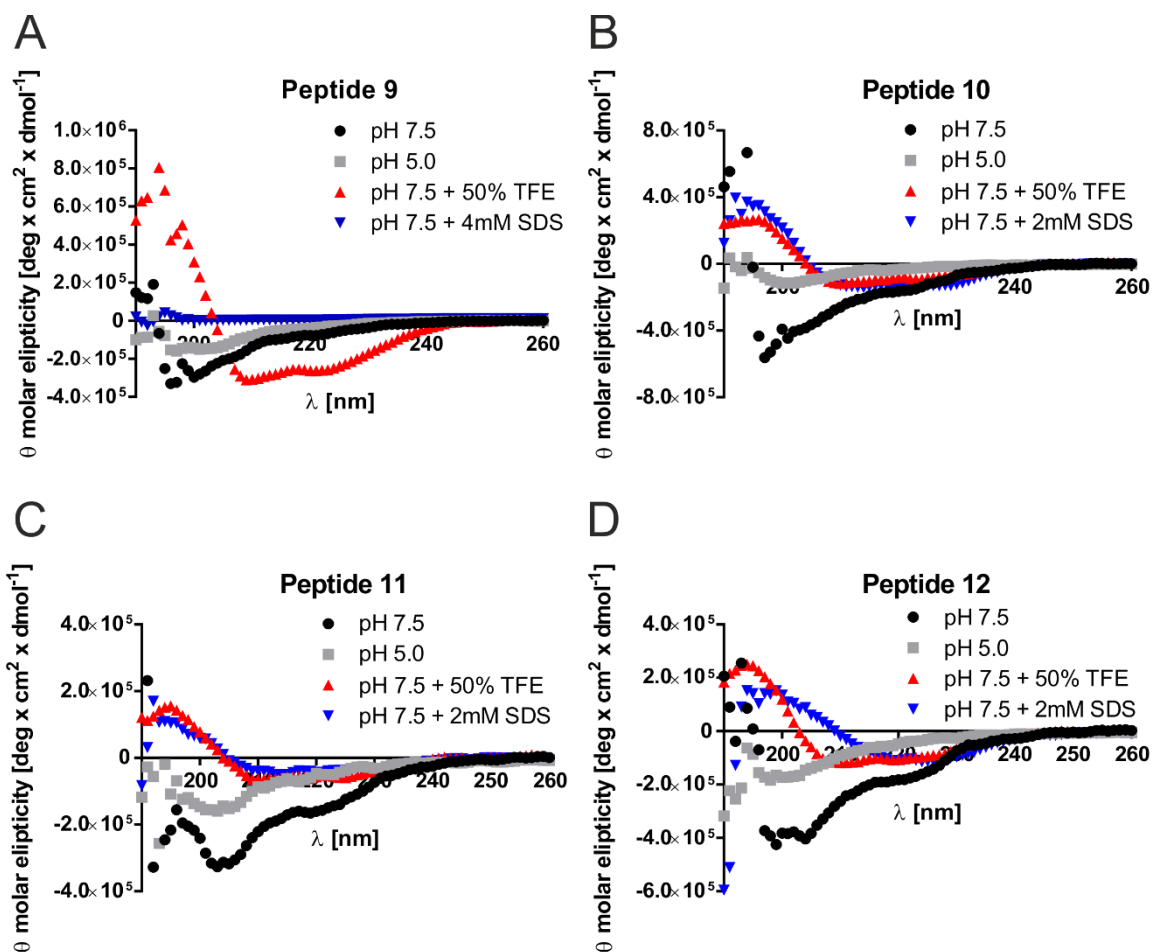


**Supporting Figure 17: Characterization of peptide 11.** Left panel: analytical C18 RP-HPLC chromatogram of purified Peptide 11, linear gradient 10-90% ACN, *baseline subtracted*. Right panel: corresponding mass spectrum of Peptide 11 at  $t = 4.9$  min, expected mass: 2906.6 Da, observed mass: 2906 Da  $[M+H]^+$ , 1454.0  $[M+2H]^{2+}$ , 969.7  $[M+3H]^{3+}$ .

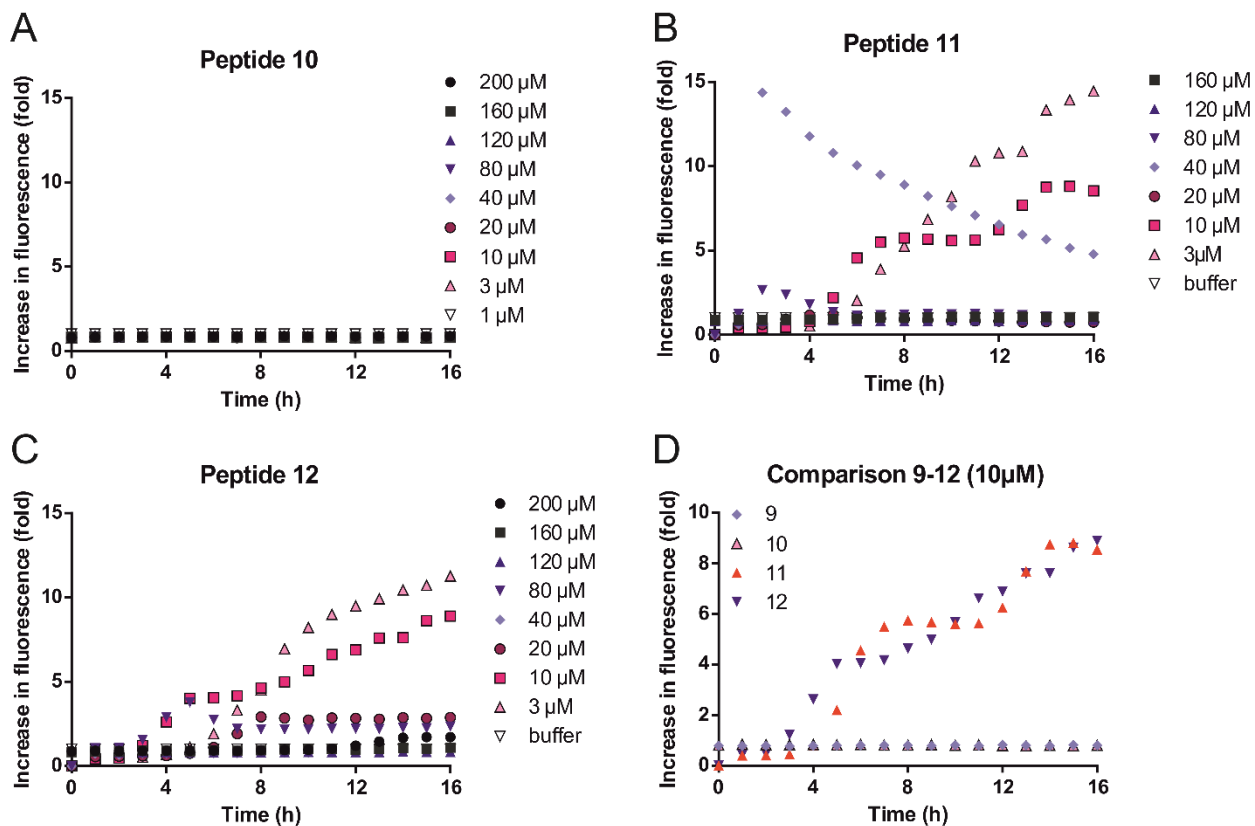


**Supporting Figure 18: Characterization of peptide 12.** Left panel: analytical C18 RP-HPLC chromatogram of purified Peptide 12, linear gradient 10-90% ACN. Right panel: corresponding mass spectrum of Peptide 12 at  $t = 4.8$  min, expected mass: 2906.6 Da, observed mass: 2906.6 Da  $[M+H]^+$ , 1454.2  $[M+2H]^{2+}$ , 969.9  $[M+3H]^{3+}$ . Additionally, TFA salt of the peptide (observed mass: 3018 Da) was obtained.

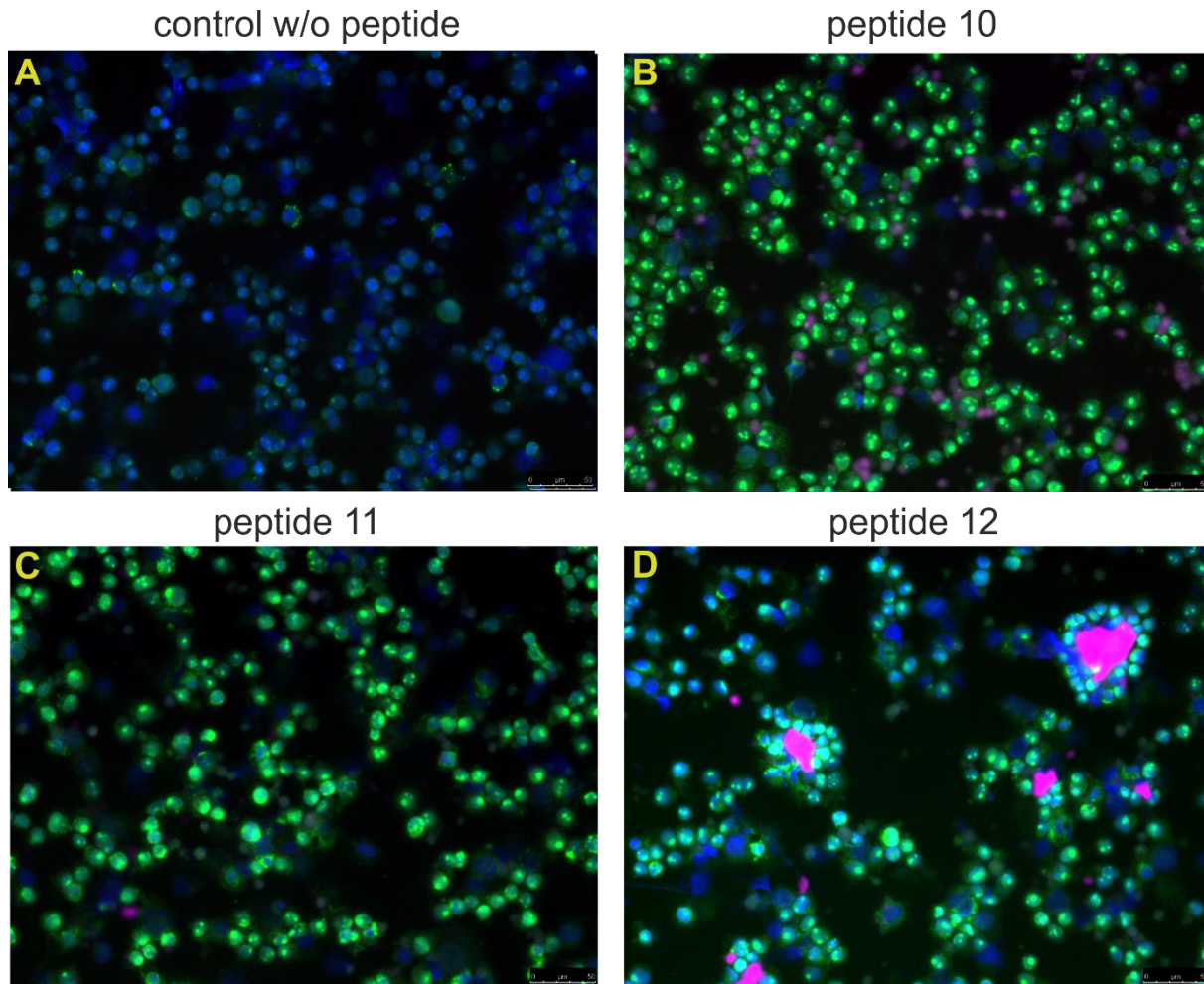




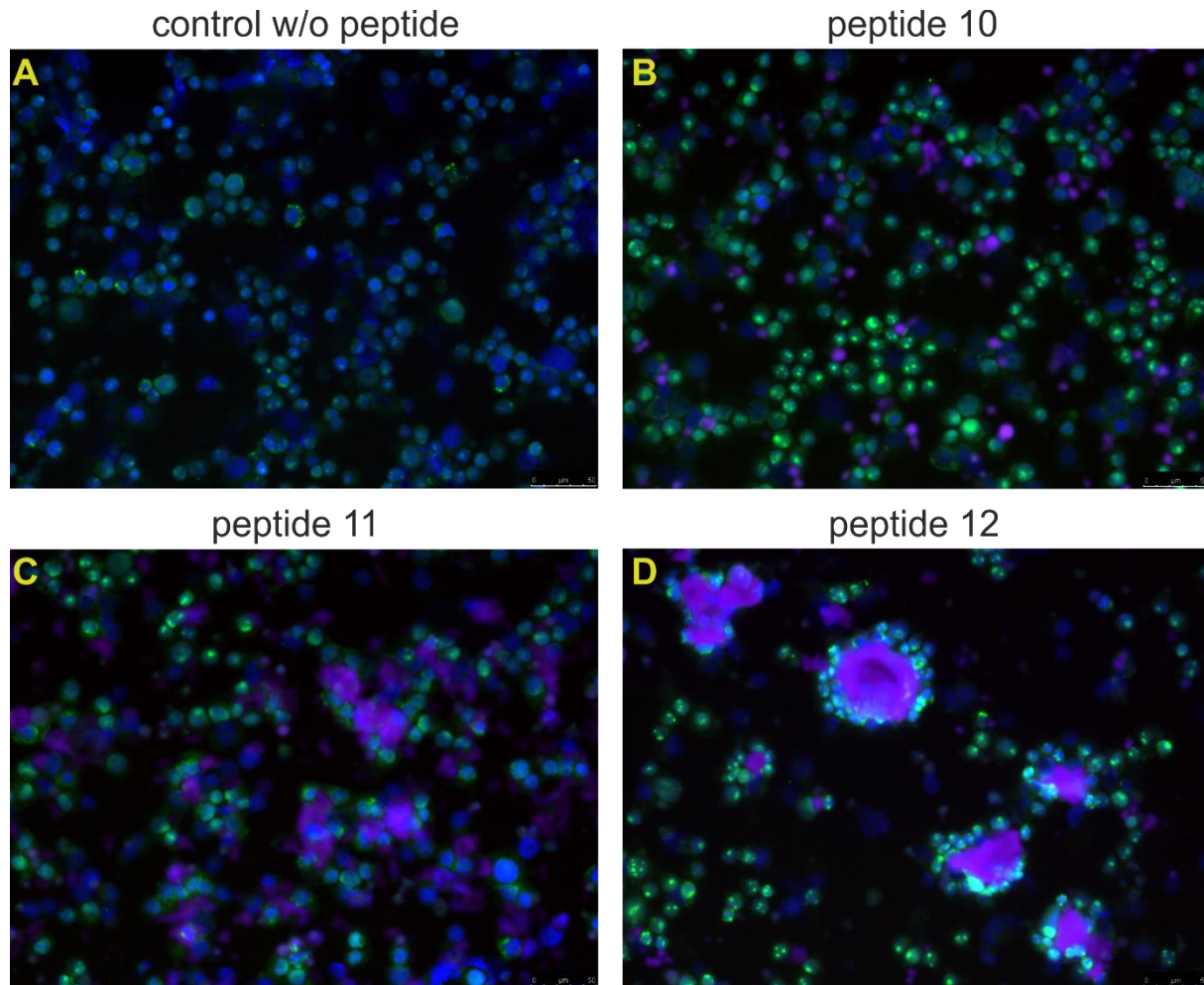
**Supporting Figure 19: Biophysical characterization of peptides 9-12 via CD spectroscopy.** All peptides were dissolved at 50  $\mu\text{M}$  concentration at pH 7.5 in 20 mM Tris buffer and the spectra were recorded as an average of 5 spectra. A-D: spectra of peptides 9-12 at different pH (5.0 and 7.5) and with additives (TFE and SDS).



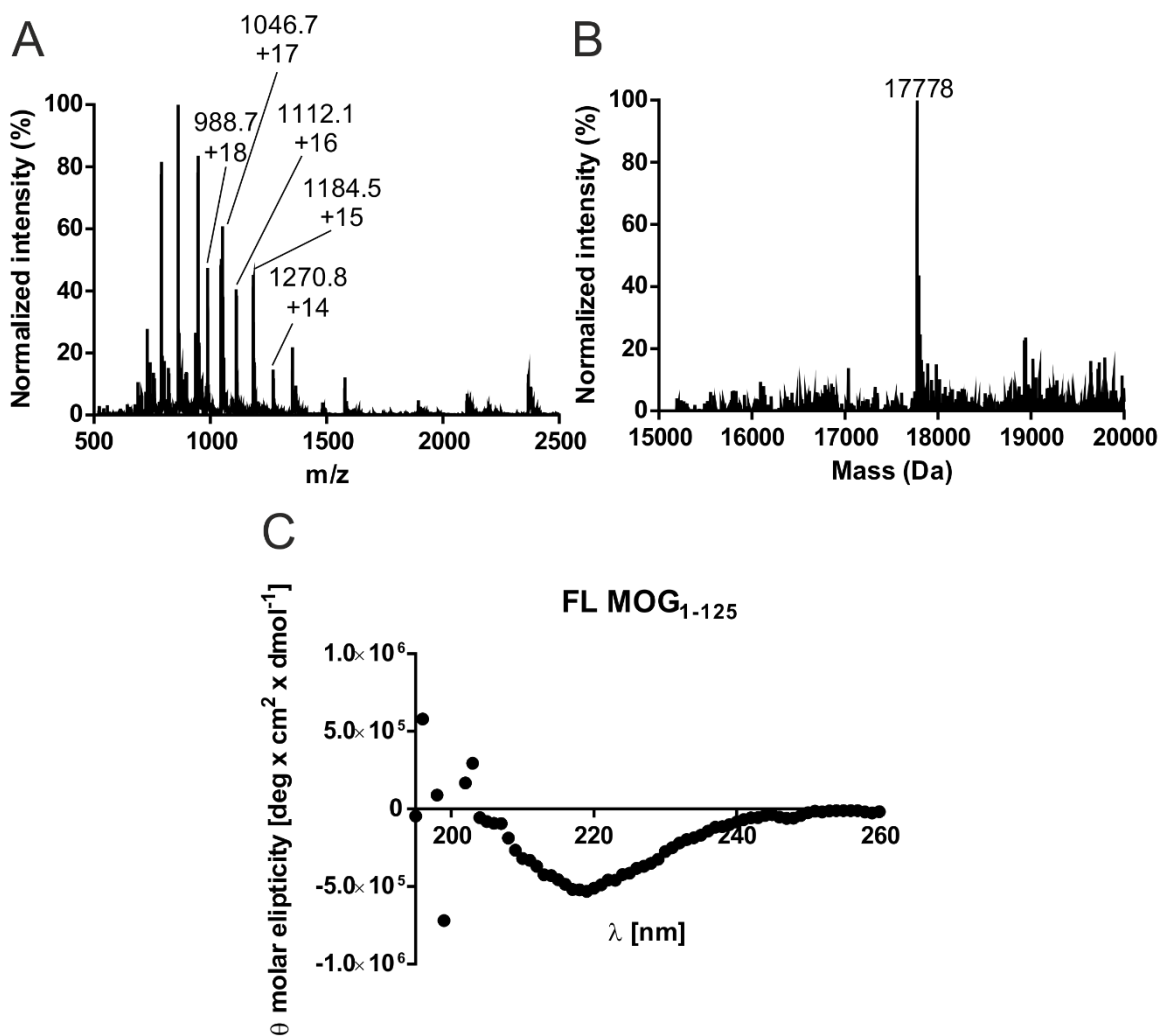
**Supporting Figure 20: ThT fluorescence of peptides 9-12 measured at 37°C, pH 5.0 at different concentrations** All data were recorded at an excitation wavelength of 444±9 nm and an emission wavelength of 485±9 nm. All samples were used at a pH of 5.0 with varying concentrations. Black circles: 200  $\mu$ M, grey squares: 160  $\mu$ M, dark blue triangle: 120  $\mu$ M, light blue triangles: 80  $\mu$ M, purple diamonds: 40  $\mu$ M, red circles: 20  $\mu$ M, red squares: 10  $\mu$ M, pink triangle: 3  $\mu$ M and white triangle: 1  $\mu$ M, A-C: fluorescence spectrum of peptides 10, 11 and 12. D: Comparison of ThT fluorescence between peptides 9-12 at 40  $\mu$ M. The fluorescence change is normalized to 20 mM NaOAc (pH 5) treated with equal amount of ThT as in the samples.



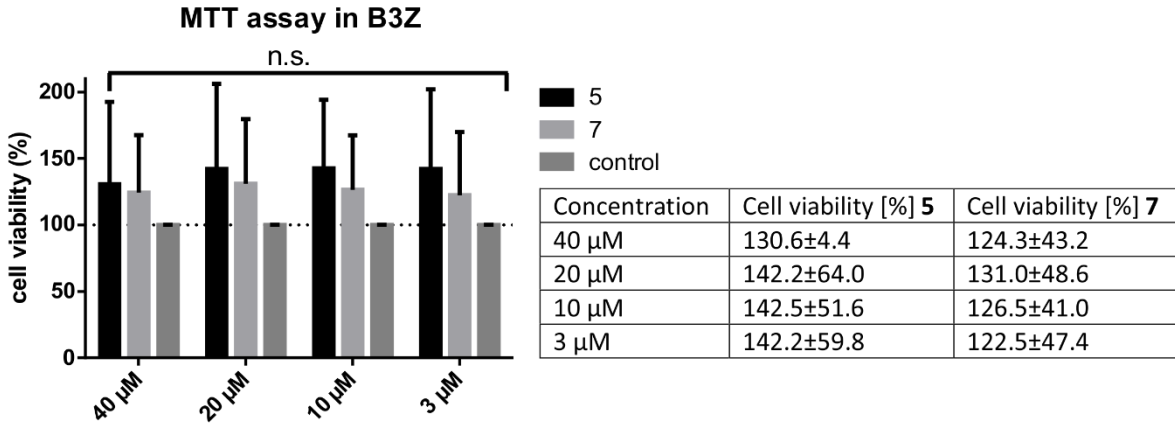
**Supplementary Figure 21: Monitoring the uptake & aggregation of bioorthogonal, site-specific citrullinated MOG peptides via confocal microscopy.** Human EBV infected B-cells were incubated 72 h with 3.125  $\mu\text{M}$  of either no peptide (A), peptide 10 (B), peptide 11 (C) or peptide 12 (D). Cells were fixed with 4% PFA and processed for immunofluorescence with following primary antibodies and dyes; the nucleus was stained with DAPI (blue) and LC-3 was used as a autophagosome marker (green). The bioorthogonal peptides were stained using CuAAC chemistry with azide Alexa-647 (Thermo Fisher, the Netherlands). Scale bar 50  $\mu\text{m}$ .



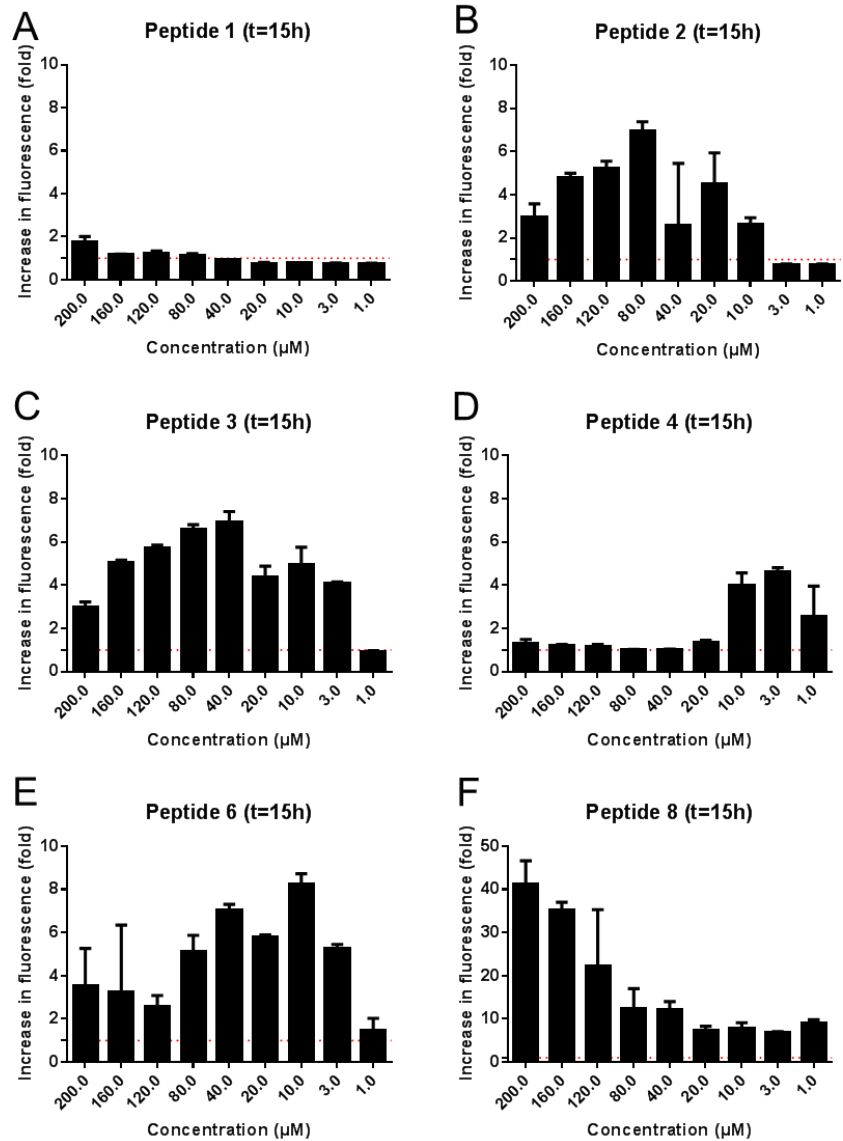
**Supplementary Figure 22: Monitoring the uptake&aggregation of bioorthogonal site-specific citrullinated MOG peptides via confocal microscopy.** Human EBV infected B-cells were incubated 72h with 12.5  $\mu$ M of either no peptide (A), peptide 10 (B), peptide 11 (C) or peptide 12 (D). Cells were fixed with 4% PFA and processed for immunofluorescence with following primary antibodies and dyes; the nucleus was stained with DAPI (blue) and LC-3 was used as a autophagosome marker (green). The bioorthogonal peptides were stained using CuAAC chemistry with azide Alexa-647 (Thermo Fisher, the Netherlands). Scale bar 50  $\mu$ m.



**Supporting Figure 23: Characterization of FL-rMOG<sub>1-125</sub>.** A) ESI-MS of FL-rMOG<sub>1-125</sub>, expected mass: 17778.2 Da, observed mass: 17778 Da [M+H]<sup>+</sup>. 18- to 14-fold multiple charged ion peaks were detected. B) Deconvoluted mass spectrum of FL-rMOG<sub>1-125</sub>, C) CD spectrum of FL-rMOG<sub>1-125</sub> (5.6 μM), the spectrum is an average of at least 5 independent measurements. The results are in good agreement with previously published work<sup>1-2</sup>.



**Supporting Figure 24: Cytotoxicity assays with citrullinated MOG peptides in B3Z hybridoma cells.** n.s. not significant. The error bars represent  $\pm$ SD, the experiment was conducted n=3 and with three biological replicates.



**Supporting Figure 25: Plotted ThT fluorescence spectra of peptides 1-4 (A-D), 6 (E) and 8 (F).** All aggregation assays were performed at least n=3 and with experimental triplicates and at time point t= 15 h representing the endpoint of aggregation kinetics.

$$Y = \frac{Bottom + (Top - Bottom)}{1 + 10^{(LogIC_{50} - X) * Hillslope}}$$

**Equation E1**

Table S1: Parameters of the sigmoidal curves interpolated with seeded aggregations of 5.

	Top	Bottom	LogIC <sub>50</sub>	Hillslope	Time at 0.9-fold (h)	Δt <sub>1/2</sub>
<b>5</b>	8.611	0.680	11.720	0.348	9.72	0.00
<b>5+0.3μg seed 5*</b>	7.473	0.78	12.900	0.343	8.00	n.s.
<b>5+0.03μg seed 5</b>	9.696	0.795	10.670	0.752	8.62	1.09
<b>p5+0.003μg seed 5</b>	5.535	0.839	10.990	0.466	8.78	0.94
<b>p5+0.3μg seed 7</b>	9.349	0.862	9.365	0.691	6.86	2.86
<b>p5+0.03μg seed 7</b>	9.254	0.727	9.433	0.694	7.59	2.13
<b>p5+0.003μg seed 7</b>	9.557	0.692	10.220	0.476	8.28	1.44

\*upon addition of 0.3 μg seeds of 5 non-significant results were obtained, which can be explained by an insufficient fitting according to E1.

Table S2: Parameters of the sigmoidal curves interpolated with seeded aggregations of 7.

	Top	Bottom	LogIC <sub>50</sub>	Hillslope	Time at 0.9-fold (h)	Δt <sub>1/2</sub>
<b>7</b>	2.636	0.676	6.790	0.287	5.36	0.00
<b>p7+0.3μg seed 5</b>	3.612	0.620	11.350	0.107	9.39	-4.03*
<b>p7+0.03μg seed 5</b>	9.437	-0.399	19.200	0.045	17.03	-11.67*
<b>p7+0.003μg seed 5</b>	3.913	-1.028	3.147	0.077	1.84	3.52
<b>p7+0.3μg seed 7</b>	3.687	0.404	5.638	0.169	4.12	1.24
<b>p7+0.03μg seed 7</b>	3.297	0.835	7.214	0.321	5.16	0.20
<b>p7+0.003μg seed 7</b>	3.359	0.595	5.864	0.214	4.29	1.07

\*addition of 0.3 μg and 0.03 μg seeds of 5 did not result in reaching a plateau phase, the negative time shift calculated can be explained by an insufficient fitting according to E1.

## References

1. Menge, T.; Lalive, P. H.; von Büdingen, H. C.; Genain, C. P., Conformational epitopes of myelin oligodendrocyte glycoprotein are targets of potentially pathogenic antibody responses in multiple sclerosis. *J. Neuroinflamm.* **2011**, *8*, 161-161.
2. Gori, F.; Mulinacci, B.; Massai, L.; Avolio, C.; Caragnano, M.; Peroni, E.; Lori, S.; Chelli, M.; Papini, A. M.; Rovero, P.; Lolli, F., IgG and IgM antibodies to the refolded MOG1–125 extracellular domain in humans. *J. Neuroimmunol.* **2011**, *233* (1), 216-220.